Lawrence Berkeley National Laboratory
Lawrence Berkeley National Laboratory

Title

Climate implications of carbonaceous aerosols: An aerosol microphysical study using the GISS/MATRIX climate model

Permalink

https://escholarship.org/uc/item/1g11497k

Author

Bauer, Susanne E.

Publication Date

2010-05-28

Peer reviewed

Climate implications of carbonaceous aerosols:

An aerosol microphysical study using the GISS/MATRIX climate model

Susanne E. Bauer[1,2], Surabi Menon[3], Dorothy Koch[1,2], Tami Bond[4] and Kostas Tsigaridis[1]

(1) NASA Goddard Institute for Space Studies, New York, NY
(2) The Earth Institute, Columbia University, New York, NY
(3) Lawrence Berkeley National Laboratory, Berkeley, CA
(4) University of Illinois, Urbana-Champaign, IL

Abstract

Recently, attention has been drawn towards black carbon aerosols as a likely short-term climate warming mitigation candidate. However the global and regional impacts of the direct, cloud-indirect and semi-direct forcing effects are highly uncertain, due to the complex nature of aerosol evolution and its climate interactions. Black carbon is directly released as particle into the atmosphere, but then interacts with other gases and particles through condensation and coagulation processes leading to further aerosol growth, aging and internal mixing. A detailed aerosol microphysical scheme, MATRIX, embedded within the global GISS modelE includes the above processes that determine the lifecycle and climate impact of aerosols. This study presents a quantitative assessment of the impact of microphysical processes involving black carbon, such as emission size distributions and optical properties on aerosol cloud activation and radiative forcing.

Our best estimate for net direct and indirect aerosol radiative forcing change is -0.56 W/m^2 between 1750 and 2000. However, the direct and indirect aerosol effects are very sensitive to the black and organic carbon size distribution and consequential mixing state. The net radiative forcing change can vary between -0.32 to -0.75 W/m^2 depending on these carbonaceous particle properties. Assuming that sulfates, nitrates and secondary organics form a coating shell around a black carbon core, rather than forming a uniformly mixed particles, changes the overall net radiative forcing from a negative to a positive number. Black carbon mitigation scenarios showed generally a benefit when mainly black carbon sources such as diesel emissions are reduced, reducing organic and black carbon sources such as bio-fuels, does not lead to reduced warming.

1. Introduction

Anthropogenic and natural aerosols impact the Earth's radiation balance and thus exert a forcing on global climate. Black carbon (BC) is one of the aerosol species that has a positive radiative forcing effect among other species that mainly lead to atmospheric cooling. Therefore generally the cleaning up of aerosols, which is much needed due to the severe health impact of those toxic air pollutants, would further strengthen the global warming trend. However mitigation of BC should more likely be beneficial in terms of mitigating both climate warming and air pollution. Emission reductions that target light-absorbing aerosol might also reduce warming quickly [Hansen et al., 2000; Jacobson, 2002; Bond and Sun, 2005]. However, BC's indirect (cloud microphysics) and semi-direct contributions to net climate forcing remain an outstanding uncertainty. For example, the model study of Penner et al. [2003] suggested that "smoke" did not produce net warming, considering both direct and cloud effects. However, model experiments are very sensitive to treatment of aerosol microphysics.

The aerosol direct effect (ADE) is caused by absorption and scattering of solar radiation by liquid and solid aerosol particles in the atmosphere. Most absorbing, and therefore enhancing climate warming, are black carbon (BC) particles. The absorbing strength of a BC particle strongly depends on the particle effective size and mixing state. Both of those quantities depend on the size and chemical composition of black carbon while it is released into the atmosphere as well as its microphysical and chemical evolution while transported through the atmosphere. Most other aerosol species, such as sulfate, nitrate, organic carbon (although some organics can be slightly absorbing), sea salt, aerosol water and to a certain extend mineral dust, mainly scatter solar radiation back to space, and therefore counterbalance climate warming, by cooling the atmosphere. The correct treatment of the aerosol size and mixing state is crucial in order to calculate their radiative forcing.

Attempts to quantify the ADE, the difference in top of the atmosphere forcing between pre-industrial and present day conditions, by the AeroCom initiative gave estimates between -0.41 and +0.04 W/m^2 [Schulz et al. 2006] and by the IPCC AR4 report a range from -0.9 to -0.1 W/m^2 [IPCC, 1007]. The wide range of uncertainty is caused on the one

hand by large discrepancies among the model systems, ranging from emission strength, transport, aerosol transformation, removal and optical properties. However the models are also poorly constrained by limited availability of aerosol measurements. Furthermore, Myhre [2009] explains large deviations between models and satellite retrieved ADE estimates by the lack of considering correct pre-industrial aerosol distributions in the satellite data derived forcing calculations and in failure to sample the model like the retrieval.

The aerosol indirect effect (AIE) is caused by enhancement of hydrophilic aerosols that are able to increase cloud droplet number concentrations, reduce cloud droplet size, increase cloud albedo (first indirect effect) and suppress precipitation and increases the cloud life time (second indirect effect), thereby cooling the planet [IPCC, 2007]. The role of BC in determining cloud droplet number concentrations (CDNC) is unknown, as it depends upon the mixing state of and configuration of BC with soluble species such as sulfate, nitrate and organic carbon. Furthermore, insoluble black carbon or dust aerosols can act as ice nuclei and therefore alter cirrus and mixed-phase clouds; however this role and its effects are poorly known [e.g. Lohmann et al. 2008]. Here again the microphysical evolution of the aerosol population in terms of size and mixing state is crucial in order to calculate which particles are suitable for cloud activation. Overall the IPCC AR4 report estimates the AIE to lie between -1.8 and -0.3 W/m^2. The AeroCom initiative, linking models to satellite-based estimates gives a range of -0.7±0.5 W/m^2 [Quaas et al. 2009]. The models on which these estimates were based generally did not include sophisticated treatment of aerosol mixing state. Furthermore the contribution of BC mixing to the AIE uncertainty could not have been properly evaluated.

In this study we are particularly interested in the microphysical evolution of black carbon. Several uncertain characteristics must be assumed or estimated based on available constraints. This starts with the question of the size and mixing state of an emitted BC particle. Once emitted, BC can grow by coagulation and condensation. Although freshly emitted pure BC is hydrophobic, inorganic and organic coatings will attract water and convert particles to be hydroscopic. Materials likely to condense on a BC particle, as on

any other particle, are sulfate and nitrate precursors as well as secondary organics. Those particles are likely to form a core – shell particle, where the insoluble BC fraction would form the core and the water-soluble species would enclose that core with a shell. Jacobson [2000] performed global simulations with core-shell treatment and found BC forcings 50% higher and 40% lower than forcings obtained with externally mixed and well-internally mixed treatments, respectively.

Other than surface condensation processes, coagulation is a very effective mixing pathway. One important question to answer is when BC coagulates with a soluble particle, such as sulfate or organics, what is the most likely shape of such a particle; would they form a core-shell type of structure or a double sphere structure? In the atmosphere every aerosol shape is unique, complex and not necessarily spherical. Transmission electron microscopy (TEM) images support the theory that BC particles become coated once emitted. Although BC may be internally mixed with other components, BC cannot be 'well-mixed' (diluted) in the particle, since soot, which contains BC, is irregularly shaped and mostly solid. Thus most likely BC is distinct and not well mixed within particles. But we have to understand how to best represent aerosol mixtures in a GCM that has a Mie-theory based radiation code such as the one used in this study.

As we mainly focus on the role of BC in aerosol forcing we will study the following questions:
How important is the size distribution of carbonaceous particles at emission time (section 3)? How sensitive are the ADE forcings with respect to the shape of mixed BC particles (section 4)? How well can we constrain our simulations with observational data (section 5)? And how are BC reduction experiments affected by the previously discussed microphysical modeling uncertainties (section 6)?

This paper is linked to a study by Menon et al. (2009)(Paper in submission to ACPD) (hereafter referred to as SM09) where the same model version and configuration as in this study is used, but the analysis is more detailed with respect to the AIE including evaluation, and comparison of the performance of the AIE between the new coupled

cloud and aerosol microphysics to the previous mass based GISS model [Koch et al 2006, Menon and Rotstayn, 2006].

2. Model description

The Goddard Institute for Space Studies (GISS) General Circulation Model (GCM) climate modelE [Schmidt et al., 2006; Hansen et al., 2005] coupled to the aerosol microphysics and chemistry model MATRIX (Multiconfiguration Aerosol TRacker of mIXing state) [Bauer et al., 2008], hereafter BA08, is used in this study. MATRIX is designed to support model calculations of the direct and indirect effect and permit detailed treatment of aerosol mixing state, size and aerosol-cloud activation.

MATRIX is based on the quadrature methods of moments, for each aerosol population, defined by mixing state and size distribution, the tracked species are number concentration, and mass concentration of sulfate, nitrate, ammonium, aerosol water, black carbon, organic carbon, mineral dust, and sea salt. Here we use the aerosol population setup called "mechanism 1" (BA08), given in Table 1. MATRIX dynamics includes nucleation, new particle formation, particle emissions, gas-particle mass transfer, aerosol phase chemistry, condensational growth, coagulation, and cloud activation. A detailed model description is provided by BA08.

New additions to BA08 are linking the aerosol scheme to a new aerosol indirect effect scheme that uses prognostic equations [Morrison and Gettelman, 2008] to calculate the cloud droplet number concentrations, as described in SM09. A further addition to BA08 is the coupling of mixed aerosol populations to the radiation scheme as described below.

2.1 Aerosol radiation coupling

Previously the GISS radiation scheme only treated externally mixed aerosol populations, suitable for our mass based aerosol scheme [Koch et al. 2006]. Here we describe the new coupling scheme for internally mixed aerosol populations. The GISS model radiation scheme [Hansen et al., 1983] includes explicit multiple scattering calculations for solar radiation [shortwave (SW)] and explicit integrations over both the SW and thermal [longwave (LW)] spectral regions. Gaseous absorbers of LW radiation are H_2O, CO_2, O_3,

O$_2$, and NO$_2$. Size dependent scattering properties of clouds and aerosols are computed from Mie scattering, ray tracing, and T-matrix theory (Mishchenko et al. 1996) to include non-spherical cirrus and dust particles. The k-distribution approach (Lacis and Oinas 1991) utilizes 15 non-contiguous spectral intervals to model overlapping cloud aerosol and gaseous absorption.

The MATRIX module calculates the optical properties, single scattering albedo, asymmetry factor and extinction for the 16 aerosol populations (see Table 1) for six wavelength bands in the SW and 33 bands in LW and passes those to the GISS radiation code. Each population can include multiple chemical species. Each aerosol population, as indicated in Table 1, is treated as an external mixture, a homogeneous internal mixture or a core-shell particle, depending on its chemical composition. If a particle only contains one chemical species, for example a freshly emitted pure organic carbon particle, then the optical properties match those of an externally mixed particle. In those cases MATRIX calculates the refractive index for each population and then uses Mie-code pre-calculated lookup tables in order to assign the corresponding optical parameters. A homogeneous internal mixture is assumed to be a well-mixed particle, most likely containing soluble species including aerosol water. MATRIX calculates the optical properties for those particles by using the volume mixing approach. Black carbon containing particles can exist in various shapes. A pure BC particle is externally mixed (part of population BC1). BC coated by condensed sulfate, nitrate, organics and aerosol water can form a core-shell particle, where the insoluble BC forms the core and the soluble material the shell. Pre-calculated lookup tables using the core-shell model by Toon and Ackerman [1981] provide optical specifications for all possible combinations of BC core sizes and shell thicknesses of various compositions formed out of sulfate, nitrate, organics and aerosol water. The following refractive indices at 550nm are used in this study: Sulfate (1.528-1.e-7i), nitrate (1.528-1.e-7i), OC (1.527-0.014i), BC (1.85-0.71i), sea salt (1.45-0.i), dust (1.564-0.002i) and water (1.334-3.91e-8i).

Here, we did not perform special optical calculations for core-shell particles involving mineral dust. This was not necessary as the potential shell thicknesses of such particles would be too thin for them to optically make any significant impact [Bauer et al 2007]. Therefore the optical properties for the populations DD1, DS1, DD2 and DS2 are close to

those of externally mixed mineral dust. However, this might not be true for the dust particles included in the mixed mode (MXX), as here mineral dust is mainly mixed with sea salt, and therefore mineral dust is not necessary the dominating species. Population MXX is treated as homogeneously internally mixed, due to the complicated mixing involving all eight components, dust, sea salt, sulfate, nitrate, ammonium, BC, OC, and water. In this study the base case simulation uses the volume mixing approach for all internally mixed particles. The impact of BC containing core shell particles is discussed separately in section 4.

2.2 Model configuration

Anthropogenic and natural emissions for present day and pre-industrial conditions are taken from the AeroCom project [Dentener et al., 2006 and http,://nansen.ipsl.juissieu.fr/AEROCOM/]. We use fluxes for "natural" emissions of dust, sea salt and dimethyl sulfide (DMS), and organic carbon (OC) assuming secondary organic aerosol as a 15% yield from terpene emissions, and in addition, anthropogenic emissions from biomass burning and fossil and bio fuel burning of SO_2, organic carbon (OC) and BC. The inventory provides data for the year 2000 (present-day conditions) and for the year 1750 (pre-industrial conditions).

Model simulations for present day and pre-industrial conditions only differ by emission levels. Present day atmospheric conditions, including present day sea surface temperature, are also applied for the pre-industrial emission runs. The model is employed on a horizontal resolution of $4° \times 5°$ latitude by longitude and 23 vertical layers. The model uses a 30 minute time step for all physics calculations. Every model simulation is integrated for 5.5 years, and if not otherwise noted, five year mean conditions are discussed in this paper.

3. Emission flux size information

In order to calculate emission fluxes in microphysical aerosol models, the mass and number concentration and the mixing state of those emissions need to be known. Information about size distributions is very important for particulate emission fluxes,

such as dust, sea salt and carbonaceous emissions. Usually some size information is provided for dust and sea salt emissions, or interactively calculated in models, but not for carbonaceous aerosols. Current emission inventories, such as Bond et al. [2004] or Cooke et al. [1999] provide only mass emission information, so that each modeler has to choose what sizes to assign for carbonaceous emission fluxes. Textor et al [2006] summarized the sizes of the emitted particles as used by 16 different models that participated in the AeroCom study. Mass median diameter ranging from 0.02 to 0.85 μm have been used for BC and OC emission. Some AeroCom models used different sizes for fossil and biomass burning sources, and some models emitted BC and OC emissions into several size bins. However these choices differed greatly among the models; furthermore there is very little information available about actual emission sizes. Bond et al (2006, Table 3.) collected particle size distribution observations at combustion sources from the literature and reports mass median diameters of 0.038 – 0.32 μm for diesel vehicles, 0.02 – 1.5 μm for gasoline vehicles, 0.001 – 1.05 μm for small solid fuel combustors, such as wood fireplaces or cooking stoves, and 0.05 – 0.78 μm for large stationary sources such as industrial boilers. However these sizes obtained close to emitters may not be appropriate for global model gridbox-scale initial particle sizes.

In order to understand the importance of emission size distribution of carbonaceous particles, we perform a series of sensitivity studies where only the emission sizes of carbonaceous emissions are varied. Note that those sizes are just the emission sizes, and that aged particle sizes are determined by the subsequent microphysical processes. In our simulations, carbonaceous aerosols roughly grow by a factor of three, through coagulation, condensation and water uptake processes. We assume that fossil and bio fuel BC and OC emissions enter the atmosphere as external mixtures, entering population BC1 and OCC, and biomass burning emissions are internally mixed, entering population BOC in our model. However the model is rather insensitive towards this assumption, as BC and OC from biomass burning sources coagulate very quickly even if emitted as external mixtures (not shown here).

The geometric mean emission particle diameters chosen for the single experiments are reported in Table 2. Three sensitivity experiments are performed around the base case simulation (BA or S2), one experiment with smaller emission sizes (S1) and, two

experiments with larger emission sizes, (S3, S4). The set of experiments covers approximately the range of observed emission sizes.

The design of the sensitivity experiments is rather simple, but analyzing the results is difficult as nearly everything in the aerosol simulation is affected. First we will analyze the differences between the base case BA and S1, the experiment with the smallest BC/OC emission sizes. Smaller carbonaceous particles in experiment S1 impact the mixing state and size distribution in all of MATRIX's populations. Size is the most important particle property affecting coagulation. The differences in sulfate, OC and BC mixing state between BA and S1 (S1–BA) are presented in Fig. 1 for present day conditions. Smaller initial OC/BC sizes lead to more coagulation between sulfate and BC. The sulfate coagulation rate to form BCS increases from 1087 (BA) to 8655 (S1) Gg/a, leaving less externally mixed sulfate in the system (sulfate ACC and AKK loads decrease from 188 (BA) to 41 Gg (S1)). This change feeds back into the sulfate primary particle production, and also decreasing sulfate nucleation rates (1800 Gg/a (BA), 1168 Gg/a (S1)), hence changes the size distribution. BC (Fig.1 row 2) itself favors coagulation with OC for S1, this however increases the sulfate ratio in the BCS population. So overall sulfate predominantly mixes with BC and BC mixes more with OC, leaving fewer externally mixed OC (OCC) in the atmosphere. Furthermore, the smaller overall OC/BC sizes leads to more coagulation of OC and BC with coarse particles. This effect is mostly seen in the change of aerosol optical thickness (AOT) between BA and S1 (see Fig. 2). Figure 2 presents the differences of experiments S1 and S3 with BA, all for present day conditions. Aerosol (direct) radiative forcing (ARF) and cloud radiative forcing (CRF) changes are shown for present day conditions. ARF is calculated by taking the difference between radtiative transfer calculations with and without aerosols. CRF is calculated from changes to the net cloud forcing obtained from differences between total and clear skies for each call to the radiation excluding aerosols.

Comparing BA and S1, AOT increases over the oceans and decreases in the biomass burning areas. The aerosol direct effect shows a similar pattern but of opposite sign. ARF increases in the BC/OC regions, due to internal mixing of BC and therefore enhancing overall BC absorption, which leads to more warming due to BC particles. However the dominating feature here is the enhanced cooling effect over the oceans, which is caused

by a strong contribution from the mixed population, MXX. The smaller particles in S1 lead to overall more mixing. If all 7 species are mixed together MXX is populated. However MXX is always representing a coarse mode as usually some sea salt or dust is present in MXX. Therefore at this point we can't be sure if the strong cooling over the ocean appears because of physical or numerical reasons.

Changes in CRF depends on particle chemistry and number concentrations, and therefore strongly on the size distribution, which might lead to different changes than seen in the mass concentrations as discussed in Fig.1. Regionally the negative or cooling CRF (Fig.2) is caused by the increased cloud droplet number concentration (CDNC) in those regions and vise versa. Most important is the shift in size and mixing state: particles are smaller and more internally mixed in S1, leading to a larger number of cloud activating particles in polluted sulfate rich regions, but to regional decreases in CDNCs in biomass burning, OC/BC rich regions. In the BASE case CDNCs in biomass burning regions are dominated by externally mixed OC, e.g. OCC, whereas in S1 more of OC is mixed with BOC leading to overall smaller number concentrations in biomass burning areas. Globally cloud-forcing increases over the oceans leading to a difference of -0.83 W/m^2 in CRF.

The second set of experiments, S3 and S4, tests the sensitivity of our model towards larger BC/OC emission sizes. Fortunately, these experiments respond in a linear fashion towards each other, so that it is sufficient here to discuss the results of case S3. Larger initial OC/BC particles lead to less internal mixing of the aerosol populations, leaving more externally mixed sulfate and OC particles in the atmosphere. Externally mixed sulfate increases from 188 Gg/a (BA) to 575 Gg/a (S4) and more sulfate condenses on coarse particles. Also OC and BC are less mixed with each other, but BC in the biomass burning regions is more mixed with sulfate, leading again to an increase of BC in the BCS population. All those impacts on mixing state are mostly just reverse to what we have discussed above for case S1, however this does not translate into a linear response for the aerosol optics (Fig. 2). AOT globally decreases due to less extinction by the slightly larger and more externally mixed particles. The direct aerosol (ARF) effect is slightly positive, with more warming in dust regions. This is caused by less coagulation with the overall larger OC/BC/SU particles with dust, hence increasing dust lifetime in

S4. CDNC particle concentrations are reduced by -15% (S3) and -20% (S4) leading to an increase in LWP (0.5%(S3) and 0.8% (S4)), increased cloud cover (1.% (S3) and 0.3% (S4)) and an weakened indirect effect by 3% (S3) and 4% (S4).

After discussing the complex interactions a simple summary (Fig. 3) can be given for the impact of carbonaceous aerosol emission sizes on radiative forcings: Smaller BC/OC emission sizes lead to larger, more cooling, direct and indirect aerosol forcings and larger BC/OC emission sizes to smaller forcings and therefore less aerosol cooling.

4. Particle mixing state and radiative transfer

Black carbons absorption depends strongly on its mixing state. It has been demonstrated in numerous publications (Fuller et al 1999, Bond and Bergstrom 2006, Lesins et al. 2002, Jacobson 2000) that when BC is treated solely as an external mixture, aerosol absorption can be underestimated by a factor of 2 to 4. We don't want to repeat these calculations external versus internal mixtures in this paper, but we want to test the difference between a homogeneous internal mixture and core-shell structured particle.

A large fraction of BC mass is mixed with other aerosol species. These internally mixed particles are either already emitted as mixtures or form a mixed particle through condensation or coagulation processes. The solubility of the involved species and the processes that lead to the formation of an internally mixed particle determines the structure of the mixed aerosol. Here we distinguish between different basic types of particles. An externally mixed particle, e.g. a dry sulfate, BC, etc particle without any coating; a homogeneously internally mixed particle of two or up to eight constituents, such as sulfate, nitrate, ammonium, OC, BC, sea salt, dust and water. In order to form a homogeneously internally mixed particle, the involved species need to be soluble. For example we would assume that an ammonium-sulfate aerosol that is coated by nitrate and OC and has taken up aerosol water could form a homogeneously mixed droplet. However, an insoluble particle, such as BC, with condensed ammonium sulfate or secondary organics material on its surface is more likely to form a core – shell particle, with one shell species, or well mixed multiple species in its shell. The core is always assumed to be at the center of the particle.

Most aerosol models that treat internally mixed aerosol populations (Stier et al, 2005) use

a volume mixing rule approach or use for example other mixing-based approaches like the Maxwell-Garnett [Garnett 1904, 1906] or Bruggeman [1935] mixing rule to calculate the optical properties of aerosols. However in this study we included core-shell model calculations, which should more accurately describe BC including particles.

In this section we will test the assumptions of homogenously internally mixed (HI) and core-shell (CS) structures of particles containing BC. The following experiments are tested:

- BASE: The volume mixing approach is used for all internally mixed aerosols.
- R1: BC coated by sulfate, nitrate, organics and water has a core – shell structure, all other particles are either externally or homogeneously internally mixed (see Tab. 1).
- R2: as R1 but only 10% of the organics are considered for coating a BC particle. The remaining 90% will be considered homogeneously internally mixed.

Fig. 4 shows the present day TOA radiative forcing for certain species and mixing states for our BASE experiment. The net aerosol forcing is -1.99 W/m^2, with contributions from externally mixed sulfates and nitrates -0.05 W/m^2 (ACC), organics -0.22 W/m^2, black carbon sulfate mixtures 0.05, BC-OC mixtures 0.05 W/m^2, mineral dust -1.45 W/m^2 and sea salt -0.62 W/m^2. Note that sea salt and dust forcing numbers are given for aerosols that mostly include sea-salt or dust, but still can be mixed with other species. Sulfate, nitrate, organic carbon, dust and sea salt lead to cooling of the atmosphere; only over the poles a positive warming appears due to the strong surface reflection. BC – sulfate (BC-SU) mixtures have positive forcing, but BC-OC mixtures have positive or negative forcing depending on the dominant mixing component, OC or BC, in the aerosol particle.

In order to understand the radiative impact of black carbon, we have to know its mixing state. The total global load of BC is 0.12 Tg, with roughly 75% of the BC mass in population BOC, therefore mixed with sulfate, nitrate and OC, and the remaining 25% are present in mixtures including sulfates and nitrates, such as population BCS, BC1, BC2 and BC3.

Figure 5 gives the fractions of BC, sulfate/nitrate, and OC (which is only included in BOC) in populations BOC and BCS. The remaining fraction is taken up by aerosol water.

Neglecting aerosol water, BC is the dominant component in population BCS, which leads to a positive radiative forcing globally. The BOC population is dominated by OC and SU. BC mass contributes only 1% on a global average, and up to 10% in biomass burning areas. The mixing state greatly influences the radiative forcing. Small BC fractions in the aerosol mixture are sufficient to result in a positive forcing (see Fig. 4), so the BOC mixture can also have a positive forcing for very small fraction of BC, for example as seen over Europe.

In simulation R1 and R2 only the optical properties of BC mixtures are changed. Therefore the radiative forcings of non- BC species remain mainly unchanged, however small changes occur due to feedbacks from the radiative forcings to the climate system. Table 3 gives global forcing numbers for BASE, R1 and R2, showing that only population BC-OC gives significantly different forcing numbers. Furthermore the differences between R1 and R2 are incidental, therefore it will be sufficient here to discuss only experiment R2. From this we learn that even coatings that resume from only 10% of the available OC mass are sufficient to change the optical properties between HI and CS significantly.

But first we will take a look at sulfate coatings. In the left column of Figure 6 the absorption optical thickness for BCS particles are displayed. BCS absorption is higher in the CS case, R2, in sulfate rich areas, and slightly lower in the biomass burning areas. Globally BCS absorption is increased by a factor of 1.1. From this we conclude that BC particles that are mainly coated by non-absorbing materials like sulfate and nitrate, the HI or CS Mie calculations give fairly similar results.

The difference between BOC and BCS particles, is that BOC particles can include on top of sulfates and nitrates as well OC. Due to the fact that OC is 10 times more abundant in the atmosphere than BC, it is not surprising to see that this leads to a much smaller BC fraction in those particles then seen for BCS (Fig. 5). The combination of a very small BC fraction and a large fraction of slightly absorbing organics in the shell leads to a large difference in absorption between the HI and CS assumption. Figure 6 shows that AAOT is enhanced by a factor of 3.3 between BASE and R2. However we were surprised to see such a strong impact on aerosol absorption, especially as several studies (Lesins et al 2006, Fuller et al. 1999) have demonstrated that absorption calculated for coated BC

13

particles are lower when they were treated as HI mixtures. To understand this behavior we plotted the percentage difference between HI and CS Mie calculations (Fig. 7) for BC / OC mixtures (left) and BC / sulfate mixtures (right). Previous studies (Fuller et al 1999, Bond and Bergstrom 2006, Lesins et al. 2002, Jacobson 2000), mainly looked at sulfate coated BC particle. For most sizes and BC mixing factions below 40% we see as well stronger absorption for HI, and therefore agree with those studies. However this is different when BC is coated by OC, which is less scattering than sulfate and slightly absorbing itself.

In our model most BOC particle radii are around 0.2 µm, and the BC faction is below 1 %. In this case we get a much stronger absorption when treating the particles as CS. However in our case this leads to such a strong positive BOC forcing (see Tab.3) that the total net radiative change between present day and pre-industrial aerosol forcing would be positive.

5. Observational constraints

The experiments performed in this study show large sensitivities of the overall aerosol simulations to the chosen carbonaceous emission sizes and towards optical particle mixing configuration assumptions. In this section the sets of sensitivity experiments are compared to observational datasets, including BC mass measurements and AERONET [Holben et al. 1998] products.

Table 4 compares the model with the averaged surface BC mass concentrations of the European EMEP (2002-2003) and the North American IMPROVE (1995-2001) network and reports the correlation coefficients. The base model underestimates European BC concentrations by a factor of 1.6. Decreasing BC emission sizes (S1 and S2) improves the simulation, but surface BC concentrations in Europe are still to low by a factor of 1.5. The model also underestimates surface BC concentrations in North America by a factor of 1.8, but with improved correlation coefficients compared to the European network. Comparing surface observations in polluted regions to a coarse 4° x 5° model is questionable, but we can conclude that the model underestimates North American and European surface concentrations. The S1 experiment leads to increased and therefore slightly improved surface concentrations in those regions.

Recent aircraft measurements provide BC profile measurements with Single Particle Soot absorption Photometers (SP2) onboard NASA and NOAA research aircrafts [Schwartz et al, 2006; Slowik et al. 2007]. The SP2 instrument uses an intense laser to heat the refractory component of individual aerosols in the accumulation mode to vaporization. The detected thermal radiation is used to determine the black carbon mass of each particle (Schwarz et al., 2006). In this paper we used the same campaign data and averaging technique as in Koch et al. [2009]. Figure 8 shows profiles measured in North American mid-latitude regions (a,d), in the tropics (b,c) and at high latitudes (e–i). The base model simulation generally agrees better with some observed profiles in the mid- and high-latitude regions, overestimates BC concentrations in the tropics and underestimates BC concentrations in some cases at high latitudes. The sensitivity experiments show a rather uniform response globally. Smaller particle size BC/OC emissions (exp. S1) increase the overall BC mass in the troposphere just while larger particles (S3,S4) leads to a decrease. However it is not possible to judge which of those simulations improves significantly the vertical distribution of BC mass concentrations, as we already get over and underestimations of BC mass concentrations in different latitude regions. Some measurements are strongly impacted by biomass burning events, which cannot be contemporaneously represented in a climate model simulation. In summary we don't see a systematic error in the vertical distribution of BC, as we have seen when compared to the surface mass measurements. However our regional observational coverage is quite limited.

The AERONET [Dubovik et al. 2002] observations are seasonally averaged for the year 2000. We use the aerosol optical thickness (AOT), which is the most reliable measurement from this network, and the absorption AOT (AAOT), the non-scattering part of the aerosol optical thickness, which involves a higher degree of uncertainty.

Figures 9 and 10 show the seasonal comparison between the AERONET data and the base model simulation. Table 4 summarizes the annual mean statistical measures for all experiments.

The simulation of AOT shows an excellent comparison with AERONET. Many seasonal and regional features are well captured, and the annual mean AOT is best represented in sensitivity experiment S1. Modeled AOT is only underestimated in some megacities,

including some European sites and in South America. The absorption optical thickness allows us to investigate the sensitivity of our model to the tested BC coating assumptions in the radiative transfer calculations, as those parameterizations change the absorbing strength of the aerosol mass before it impacts through feedbacks everything else in the climate model. Again the model shows an excellent comparison to AERONET AAOT, with a slight tendency in the base simulation to underestimate AAOT. Modeled AAOT shows globally a low bias during the NH winter season, and too low values in megacities. Having either smaller BC particles (S1) improves the simulation, but having coated BC particles (R1, R2) clearly overestimates model absorption.

In summary we learned from this evaluation that BC surface mass concentrations are systematically underestimated in Europe and the US, but the vertical distributions over the North American continent does not show a systematical bias. Aerosol optical measures, such as AOT and AAOT are fairly well simulated, and get even better assuming smaller BC particles. Larger BC particles (experiments S3 and S4) or extremely strong absorbing BC (R1, R2) worsen the simulation. Mineral dust is an important absorber and also impacts the comparison of this study however we have not carefully examined these effects here.

6. Black carbon reduction experiments

Recently, attention has been drawn towards black carbon aerosols as a likely short-term climate warming mitigation candidate. However it is questionable if these measures will be successful, because of the high uncertainty of global and regional impacts of the direct and especially the indirect aerosol forcing effects, due to the complex nature of aerosol evolution and its climate interactions. Furthermore, practically BC emission reductions would be archived by controlling certain source sectors, therefore eventually co-emitted species would be altered as well. Here we represent two idealized experiments where we simply reduce BC emissions from fossil and biofuel burning by 50% (BC_50), and a scenario where BC fossil fuel emissions are reduced by 100% (BC_BCFF). We also test two more 'realistic' cases where both, OC and BC from biofuel sources are reduced by

50% (BCOCBF), and a scenario were diesel BC and OC emissions were removed (BC_diesel). See Table 5 for emission budgets. The BC reduction experiments are performed under present day conditions and are compared to PD to PI changes of the BASE experiment. Biomass burning emissions for PD runs are 3 Tg/a BC and 34.2 Tg/a OC. Note that also the non-biomass burning OC emissions levels are effected in experiment BCOCBF and BC_diesel.

The results of all BC reduction experiments are summarized in Table 5 and Figure 11. In all experiments reducing BC emissions leads to less positive direct aerosol forcing ranging from -0.05 to -0.15 W/m^2. BC_50 and BCFF show very similar results for the direct forcing, whereas BCOCBF and BC_diesel show much weaker effects. This is caused in the diesel case by overall smaller BC emission changes as well by a slight decrease in OC emissions. In the BCOCBF case some of the cooling that is archived by the BC emission reduction is counterbalanced by the warming caused by the reduced co-emitted OC emissions. In both cases the reduced OC emissions over Europe and the US lead to reduced (BC_diesel) or diminishing (BCOCBF) BC mitigation effects in those regions, whereas in Asia and the high latitudes both measures would lead to a weakening of the positive direct aerosol forcing.

In order to understand the changes in cloud forcing Table 5 and Fig. 11 gives the respective changes in cloud diagnostics. Reducing BC emissions leads to a slight increase in CDNCs in all experiments, except BCOCBF. Reduced CDNCs are caused by the change in mixing state. Reducing the number concentration of BC particles leads to less internally mixed BC-sulfate particles, and therefore to an increase in the number concentrations of externally mixed sulfate particles, which serve very effectively as CDNC.

First we will discuss the experiments with overall reduced CDNCs, BC_50, BCFF, and BC_diesel. Regionally, for example over Europe where we see the strongest change in CDNCs, more CDNCs lead to more cloud cover and therefore to a negative cloud forcing. However, globally, more CDNCs lead to less cloud cover and eventually to positive and negative CRFs ranging from 0.11 to -0.05 W/m^2 per experiment. These opposite signs in cloud cover change are caused by indirect and semi-direct effects. Fig.

11 shows the surface forcing changes in the single experiments. Reduced BC loads leads to surface heating, due to the missing absorbers in the atmosphere. More radiation can reach and warm the Earth surface, heat the atmosphere and lead to a decrease of low-cloud cover and LWP, leading to a positive cloud radiative forcing, and therefore limiting the indirect effect if CDNC changes are small.

Case BCOCBF, where BC as well as OC emissions are reduced, shows a decrease in CDNCs. Less CDNCs, leads to reduced LWP and cloud cover and therefore logically to a smaller overall cloud forcing, resulting in an IE of 0.2 W/m^2 compared to the BASE case. The success of BC mitigation strategies depends on the combination of direct and indirect effects, the net radiative forcing. As a reference, our model produces a net forcing changes of -0.54 W/m^2 for PD – PI. Our simple BC mitigation scenarios, BC_50 and BCFF, show an increase in aerosol cooling and therefore slower global warming by -0.03 and -0.19 W/m^2. The two more 'realistic' scenarios show that mitigating diesel emissions will also slow global warming by -0.1 W/m^2, whereas reducing biofuel sources would even accelerate global warming, due to the combined reduction of BC and OC emissions.

8. Conclusions

In this paper we studied the sensitivity of BC effects on climate forcings with a climate model including detailed microphysical processes. In addition to BA08, MATRIX internally and externally mixed aerosol populations are now coupled to the radiation scheme, by explicitly taking into account core-shell structures, and to cloud indirect effects (SM09). We examine single processes and particle properties and look at their impacts on cloud and aerosol forcings. This study allows us to decide which processes need to be further studied, and what observational data are needed. First we discussed the importance of initial size distributions for particulate emissions such as BC and OC. Evaluating the model with ambient BC and AERONET measurements leads to the conclusion that best results are seen when BC/OC emission sizes are assumed to be between 0.01 and 0.0.5 μm. Aerosol microphysical models such as MATRIX now require particulate emission inventories that include information about aerosol mass, number, surface area, composition, and mixing state, and possibly including subgrid scale

effects, such as plume mixing etc, that can not be treated by current climate models.

Koch et al. [2009] showed that the previous generation of aerosol models without aerosol microphysics and mixing state influencing optical properties generally underestimate AAOT. In contrast, this study demonstrated a greatly improved agreement with retrieved AAOT, as the internal mixing of BC enhances absorption. On the other hand, Koch et al. (2009) found that these older models generally did not underestimate BC surface concentration; the rapid BC aging of the microphysical scheme in our model caused faster washout near source regions and consequent underestimation of BC surface concentrations. Thus it seems that the microphysics required to improve BC optical properties has excessively reduced model BC surface concentrations. Careful examination of regional tendencies may help resolve the new discrepancy.

We found extremely large differences in aerosol radiative forcing amounts when testing different BC mixing configuration assumptions when internally mixed with other species. In the extreme case, assuming all internally mixed OC would form a shell structure around BC, the net anthropogenic aerosol forcing would be positive. Simply assuming volume mixing rules for internally mixed particles is physically not realistic, but we found that for mainly sulfate coated BC particles the calculations using a simple volume mixing treatment are close to the more complex core-shell calculations. However, we found large differences between the assumed mixing states, homogeneously mixed or core-shell, when OC was coating a BC particle. Absorption can be amplified by a factor of 3 when BC cores only take up 1% or less of the particle volume. In our model this is mostly the case in the BC-OC population we simulate. However we doubt that this is realistic, as comparisons to AeroNet absorption showed that our core-shell simulations overestimate absorption. We assume that the Ton and Ackerman model is correct even for such small inclusions of BC, but we suspect that in the real atmosphere such small BC fractions within an particle might be unrealistic. However in order to better understand this behavior we will need to better evaluate the mixing state simulations of our model. The largest volume fraction is taken up by aerosol water, a quantity that is hardly validated in aerosol models.

In order to determine the potential geometry of an internally mixed BC particle we speculate that it may be important to understand how the particle was formed. Surface condensation of sulfate, nitrate, ammonium and aerosol water is likely to form a core-shell particle. But in order to know how much of organic species could form a coating we need to include the explicit treatment of secondary organic aerosols in the model. The implementation of an SOA module into MATRIX is under development. We conclude that chemical and morphological analysis of different individual particles is needed, along with size selective bulk analysis, to understand such processes taking into account aerosol microphysical processes.

One possible approach to observe mixing state including BC coating estimates was discussed by Shiraiwa et al. [2008], where the mixing state of BC in Asian air masses was examined by a combination of aerosol mass spectroscopy (AMS) and single-particle soot photometer SP2 data. The AMS data provide a detailed chemical analysis of the measured species, and the SP2 was able to measure the size distribution, and the mixing state of BC. Shiraiwa et al. [2008] found a median value of the shell/core diameter ratio increased to 1.6 in Asian continental and maritime air masses with a core diameter of 200 nm, while in free tropospheric and in Japanese air masses it was 1.3 − 1.4. It was estimated that internal mixing enhanced the BC absorption by a factor of 1.5 − 1.6 compared to external mixing. The calculated absorption coefficient was 2 − 3 times higher in Asian continental air masses than in clean air. A further approach would be the combination of AMS with single particle mass spectroscopy ATOF-MS (Prather et al, 1994), or chemical ionization mass spectroscopy, CIMS (Hearn and Smith, 2004) data. Our ongoing research will focus on the validation of mixing state with these newly emerging datasets.

In light of the analysed model sensitivities towards microphysical BC characterization, we perfomed a set of BC mitigation studies. In summary we learned that BC mitigation is always beneficial if only BC sources are reduced, as the direct radiative forcing is lowered, and the effects on clouds are weak. BC mitigation led to enhanced CDNC production, therefore not weakening the indirect effect. Actually semi-direct effects,

induced by changed vertical heating profiles in the atmosphere, seem to be important in our model as well as the first and second indirect effect when BC is changed. The two more 'realistic' scenarios show that mitigating diesel emissions will slow global warming by -0.1 W/m^2, whereas reducing biofuel sources would even accelerate global warming, due to the combined reduction of BC and OC emissions.

This study did not include ice cloud feedbacks or BC-snow ice albedo feedbacks (Koch et al. 2009) that may enhance warming. Despite the various limitations explored in this study regarding emission sizes and mixing state of BC particles we suggest that a reduction in BC diesel emissions would help reduce the positive forcing from BC particles. However, we stress that strategies that include a reduction in BC emissions should not delay any GHG reduction plans, as the likely reductions in positive forcing from BC emissions are small und uncertain (from +0.12 up to -0.19W/m^2) compared to GHG forcings of 2.7 (W/m^2). Furthermore, BC reductions can never be isolated from reductions of co-emitted species, many of which have negative forcings, such as OC and sulfate. However, in all cases black carbon mitigation is beneficial, but aerosol microphysical processes need to be better constrained in order to estimate how effective those measures can be.

References

Ackerman, A. S., O. B. Toon, D. E. Stevens, A. J. Heymsfield, V. Ramanathan, and E. J. Welton (2000), Reduction of tropical cloudiness by soot, Science, 288, 1042 – 1047, doi:10.1126/science.288.5468.1042.

Bauer, S.E., D. Wright, D. Koch, E. Lewis, R. McGraw, L.-S. Chang, S. Schwartz and R. Ruedy, Matrix (multiconfiguration aerosol tracker of mixing state): An aerosol microphysical module for global atmospheric models., Atmos. Chem. Phys, 8, 6603–6035, 2008.

Bauer, S.E., M.I. Mishchenko, A.A. Lacis, S. Zhang, Ja. Perlwitz, and S.M. Metzger, 2007: Do sulfate and nitrate coatings on mineral dust have important effects on radiative properties and climate modeling? J. Geophys. Res., 112, D06307, doi:10.1029/2005JD006977.

Bond, T., Streets, D., Yarber, K., Nelson, S., Wo, J.-H., and Klimont, Z.: A technology-based global inventory of black and organic carbon emissions from combustion, J. Geophys. Res., 109, D14203, doi:10.1029/2003JD003697, 2004.

Bond, T.C. and R.W. Bergstrom, (2006), Light absorption by carbonaceous particles: An investigative review, Aerosol Sci. Technol., Vol. 40, 27-67.

Bond, T.C., and H. Sun (2005), Can reducing black carbon emissions counteract global warming?, *Environ. Sci. Tech.*, *39*, 5921-5926.

Boucher, O., Moulin, C., Belviso, S., Aumont, O., Bopp, L., Cosme, E., von Kuhlmann, R., Lawrence, M. G., Pham, M., Reddy, M. S., Sciare, J., and Venkataraman, C.: DMS atmospheric concentrations and sulphate aerosol indirect radiative forcing: a sensitivity study to the DMS source representation and oxidation, Atmos. Chem. Phys., 3, 49–65, 2003, http://www.atmos-chem-phys.net/3/49/2003/.

Bruggeman, D.: Calculation of various physics constants in heterogenous substances i dielectricity constants and conductivity of mixed bodies from isotropic substances, Annalen der Physik, 24, 636–664, 1935.

Clarke, A.D., C. McNaughton, V.N. Kapustin, Y. Shinozuka, S. Howell, J. Dibb, J. Zhou, B. Anderson, V. Brekhovskikh, H. Turner, and M. Pinkerton, Biomass burning and pollution aerosol over North America: Organic components and their influence on spectral optical properties and humidification response, *J. Geophys. Res.*, *112* (D12S18), doi:10.1029/2006JD007777, 2007.

Cooke, W. F., Liousse, C., Cachier, H., and Feichter, J.: Construction of a 1x1 fossil fuel emission data set for carbonaceous aerosol and implementation and radiative impact in the ECHAM4 model, J. Geophys. Res., 104, 22 137–22 162, 1999.

Dentener, F., Kinne, S., Bond, T., Boucher, O., Cofala, J., Generos, S., Ginoux, P., Gong, S., Hoelzemann, J. J., Ito, A., Marelli, L., Penner, J., Putaud, J.-P., Textor, C., Schulz, M., v. d.Werf, G. R., andWilson, J.: Emissions of primary aerosol and precursor gases for the years 2000 and

1750 prescribed data-sets for AeroCom, Atmos. Chem. Phys., 6, 4321–4344, 2006, http://www.atmos-chem-phys.net/6/4321/2006/.

Dubovik, O., B. Holben, T. F. Eck, A. Smirnov, Y. Kaufman, M. D. King, D. Tanre, and I. Slutsker, 2002: Variability of absorption and optical properties of key aerosol types observed in worldwide locations, J. Atmos. Sci., 59, 590-608.

Fuller, K. A., Malm, W. C., and Kreidenweis, S. M. (1999). Effects of Mixing on Extinction By Carbonaceous Particles, *J. Geophys. Res. 104 (D13)*:15941– 15954.

Garnett, J.: Colours in metal glasses and in metallic films, Philos. Trans. R. Soc. London, 203, 385–420, 1904.

Garnett, J. C. M.: Colours in metal glasses, in metallic films, and in metallic solutions – II, Philos. Trans. R. Soc. London, 205, 237–288, 1906.

Gong, S. L.: A parameterization of sea-salt aerosol source function for sub- and super- micron particles, Global Biogeochemical Cycles, 17(4), 1097, doi:1029/2003GB002079, 2003.

Hansen, J. E, G. L. Russell, D. Rind, P. Stone, A. Lacis, R. Ruedy, and L. Travis, 1983: Efficient three-dimensional models for climatic studies. *Mon. Wea. Rev.,* **111,** 609–662.

Hansen, J., M. Sato, and R. Ruedy (1997), Radiative forcing and climate response, J. Geophys. Res., 102, 6831 – 6864, doi:10.1029/96JD03436.

Hansen, J., M. Sato, R. Ruedy, L. Nazarenko, A. Lacis, G. Schmidt, G. Russell, I. Aleinov, M. Bauer, S. Bauer, N. Bell, B. Cairns, V. Canuto, Y. Cheng, A. D. Genio, G. Faluvegi, E. Fleming, A. Friend, T. Hall, C. Jackman, M. Kelley, N. Kiang, D. Koch, J. Lean, J. Lerner, K. Lo, S. Menon, R. Miller, P. Minnis, T. Novakov, V. Oinas, J. Perlwitz, J. Perlwitz, D. Rind, D. Romanou, D. Shindell, P. Stone, S. Sun, N. Tausnev, D. Thresher, B. Wielicki, T. Wong, M. Yao, and S. Zhang, Efficacy of climate forcing, J. Geophys. Res, 110 (D18104), doi:10.1029/2005JD005,776, 2005.

Hansen, J., Mki. Sato, R. Ruedy, A. Lacis, and V. Oinas, 2000: Global warming in the twenty-first century: An alternative scenario. Proc. Natl. Acad. Sci., 97, 9875-9880, doi:10.1073/pnas.170278997.

Hearn,J. D. and G. D. Smith: A chemical ionization mass spectrometry method for the online analysis of organic aerosols, *Analytical Chemistry*, *76* (10), 2820-2826, 2004.

Holben, B. N., et al., 1998: AERONET—A federated instrument network and data archive for aerosol characterization, Remote Sens. Environ., 66, 1 –16.

Howell, S.G., A.D. Clarke, Y. Shinozuka, V.N. Kapustin, C.S. McNaughton, B.J. Huebert, S. Doherty, and T. Anderson, The Influence of relative humidity upon pollution and dust during ACE-Asia: size distributions and implications for optical properties, *J. Geophys. Res.*, *111* (D06205, doi:10.1029/2004JD005759), 2006.

Intergovernmental Panel on Climate Change (IPCC) Fourth Assessment Report, Climate Change 2007 Synthesis Report, Contribution of Working Groups I, II and III to the Fourth Assessment Report of the Intergovernmental Panel on Climate Change.

Jacobson, M. Z., A physically-based treatment of elemental carbon optics: Implications for global direct forcing of aerosols, Geophys. Res. Lett., 27, 217-220, 2000.

Jacobson, M.Z. (2002), Control of fossil-fuel particulate black carbon and organic matter, possibly the most effective method of slowing global warming, *J. Geophys. Res.*, *107* (D19), doi:10.1029/2001JD001376.

Koch, D., G.A. Schmidt, and C.V. Field, 2006: Sulfur, sea salt and radionuclide aerosols in GISS ModelE. *J. Geophys. Res.*, **111**, D06206, doi:10.1029/2004JD005550.

Koch D, Schulz M., S. Kinne, T. C. Bond, Y. Balkanski, S. Bauer, T. Berntsen, O. Boucher, M. Chin, A. Clarke, N. De Luca, F. Dentener, T. Diehl, O. Dubovik, R. Easter, D. W. Fahey, J. Feichter, D. Fillmore, S. Freitag, S. Ghan, P. Ginoux, S. Gong, L. Horowitz, T. Iversen, A. Kirkevåg, Z. Klimont, Y. Kondo, M. Krol, X. Liu, C. McNaughton, R. Miller, V. Montanaro, N. Moteki, G. Myhre, J. E. Penner, Ja. Perlwitz, G. Pitari, S. Reddy, L. Sahu, H. Sakamoto, G. Schuster, J. P. Schwarz, Ø. Seland, J. R. Spackman, P. Stier, N. Takegawa, T. Takemura, C. Textor, J. A. van Aardenne, and Y. Zhao: Evaluation of Black Carbon Estimations in Global Aerosol Models, Atmos. Chem. Phys. Discuss., 9, 15769-15825, 2009

Lacis, A. A., and V. Oinas, 1991: A description of the correlated k distribution method for modeling nongray gaseous absorption, thermal emission and multiple scattering in vertically inhomogeneous atmospheres. *J. Geophys. Res.,* **96,** 9027–9063.

Lesins, G., Chylek, P., and Lohmann, U. (2002). A Study of Internal and External Mixing Scenarios and Its Effect on Aerosol Optical Properties and Direct Radiative Forcing, *J. Geophys. Res.* 107(D10):4094.

Lohmann, U., Spichtinger, P., Jess, S., Peter, T., and Smit, H.: Cirrus cloud formation and ice su-persaturated regions in a global climate model, Env. Res. Lett., 3, 045022, doi:10.1088/1748-9326/3/4/045022, 2008.

McNaughton, C.S., A.D. Clarke, V.N. Kapustin, Y. Shinozuka, S.G. Howell, B.E. Anderson, E. Winstead, J. Dibb, E. Scheuer, R.C. Cohen, P.J. Wooldridge, A.E. Perring, L.G. Huey, S. Kim, J.L. Jimenez, E.J. Dunlea, E.H. DeCarlo, P.O. Wennberg, J.D. Crounse, A.J. Weinheimer, and F.M. Flocke, Observations of heterogeneous reactions between Asian pollution and mineral dust over the Eastern North Pacific during INTEX-B, *Atmospheric Chemistry and Physics Discussions*, *9* (2), 8469-8539, 2009.

Morrison H. and A. Gettelman, A new two-moment bulk stratiform cloud microphysics scheme in the Community Atmospheric Model (CAM3), Part I: Description and Numerical Tests J. Climate, 21:15, 3642-3659, 2008.
Moteki, N., and Y. Kondo, Effects of mixing state on black carbon measurement by Laser-Induced Incandescence, *Aerosol Science and Technology*, *41*, 398-417, 2007.

Moteki, N., Y. Kondo, Y. Miyazaki, N. Takegawa, Y. Komazaki, G. Kurata, T. Shirai, D.R. Blake, T. Miyakawa, and M. Koike, Evolution of mixing state of black carbon particles: Aircraft measurements over the western Pacific in March 2004, *Geophysical Research Letters*, *34* (L11803), doi:10.1029/2006GL028943, 2007.

Menon S., Bauer, S.E., Sednev I., Koch D., Morrison H., and DeMott P., 2009: Aerosol-climate interactions: Evaluation of cloud processes and regional climate impacts from varying GHG and aerosol amounts. Submitted to ACP.

Menon, S. and L. Rotstayn, 2006: The radiative influence of aerosol e•ects on liquidphase cumulus and stratiform clouds based on sensitivity studies with two climate models, Climate Dynamics, 27, 345-356, DOI 10.1007/s00382-006-0139-3.

Myhre G: Consistency between satellite-derived and modeled estimates of the direct aerosol effect, Science, Vol 325, p 187-190, 2009

Miller, R. L., Cakmur, R., Perlwitz, J., Geogdzhayev, I., Ginoux, P., Kohfeld, K., Koch, D., Prigent, C., Ruedy, R., Schmidt, G., and Tegen, I.: Mineral dust aerosols in the NASA Goddard Institute for Space Sciences ModelE atmospheric general circulation model, J. Geophys. Res., 111, D06208, doi:10.1029/2005JD005 796, 2006.

Mishchenko, M. I., L. D. Travis, and D. W. Mackowski, 1996: Tmatrix computations of light scattering by nonspherical particles:
A review. *J. Quant. Spectrosc. Radiat. Transfer,* **55,** 535–575.

Penner, J.E., S.Y. Zhang, and C.C. Chuang (2003), Soot and smoke aerosol may not warm climate, *J. Geophys. Res.*, *108* (D21), 4657, doi:10.1029/2003JD003409.

Prather, K. A., T. Nordmeyer, and K. Salt: Real-Time Characterization of Individual Aerosol-Particles Using Time-Of-Flight Mass-Spectrometry, *Analytical Chemistry*, *66* (9), 1403-1407, 1994.

Schulz, M., C. Textor, S. Kinne, Y. Balkanski, S. Bauer, T. Berntsen, T. Berglen, O. Boucher, F. Dentener, S. Guibert, I.S.A. Isaksen, T. Iversen, D. Koch, A. Kirkevåg, X. Liu, V. Montanaro, G. Myhre, J.E. Penner, G. Pitari, S. Reddy, Ø. Seland, P. Stier, and T. Takemura, 2006: Radiative forcing by aerosols as derived from the AeroCom present-day and pre-industrial simulations. Atmos. Chem. Phys., 6, 5225-5246.

Schmidt, G. A., R. Ruedy, J. Hansen, I. Aleinov, N. Bell, M. Bauer, S. Bauer, B. Cairns, Y. Cheng, A. DelGenio, G. Faluvegi, A. Friend, T. M. Hall, Y. Hu, M. Kelley, N. Kiang, D. Koch, A. A. Lacis, J. Lerner, K. K. Lo, R. L. Miller, L. Nazarenko, V. Oinas, J. Perlwitz, J. Perlwitz, D. Rind, A. Romanou, G. L. Russell, D. T. Shindell, P. H. Stone, S. Sun, N. Tausnev, and M.-S. Yao, Present day atmospheric simulations using giss modele: Comparison to in-situ, satellite and reanalysis data, J. Climate, 19, 153– 192, 2006.

Schuster, G. L., O. Dubovik, B. N. Holben, E. E. Clothiaux, 2005, Inferring black carbon content and specific absorption from Aerosol Robotic Network (AERONET) aerosol retrievals, J. Geophys. Res., 110, D10S17, doi:10.1029/2004JD004548,.

Schwarz, J. P., *et al.,* 2006: Single-particle measurements of midlatitude black carbon and lightscattering aerosols from the boundary layer to the lower stratosphere, *J. Geophys. Res., 111,* D16207.

Schwarz, J. P., et al., 2008: Coatings and their enhancement of black carbon light absorption in the tropical atmosphere, *J. Geophys. Res., 113*, D03203.

Shinozuka, Y., A.D. Clarke, S.G. Howell, V.N. Kapustin, C.S. McNaughton, J. Zhou, and B.E. Anderson, Aircraft profiles of aerosol microphysics and optical properties over North America: Aerosol optical depth and its association with PM2.5 and water uptake, *Journal of Geophysical Research*, *112* (D12S20), doi: 10.1029/2006JD007918, 2007.

Shiraiwa, M., Y. Kondo, N. Moteki, N. Takegawa, L. K. Sahu, A. Takami, S. Hatakeyama, S. Yonemura, and D. R. Blake (2008), Radiative impact of mixing state of black carbon aerosol in Asian outflow, J. Geophys. Res., 113, D24210, doi:10.1029/2008JD010546.

Slowik, J. G., *et al.* (2007)*,* An intercomparison of instruments measuring black carbon content of soot particles, *Aerosol Sci. Technol., 41*, 295.

Stier, P., J. Feichter, S. Kinne , S. Kloster , E. Vignati , J. Wilson , L. Ganzeveld , I. Tegen , M. Werner , Y. Balkanski , M. Schulz, O. Boucher, A. Minikin , and A. Petzold (2005) The aerosol-climate model ECHAM5-HAM, Atmos. Chem. Phys., 5, 1125–1156, 2005

Textor, C., M. Schulz, S. Guibert, S. Kinne, Y. Balkanski, S. Bauer, T. Berntsen, T. Berglen, O. Boucher, M. Chin, F. Dentener, T. Diehl, J. Feichter, D. Fillmore, P. Ginoux, S. Gong, A. Grini, J. Hendricks, L. Horowitz, P. Huang, I. Isaksen, T. Iversen, S. Kloster, D. Koch, A. Kirkevg, J. Kristjaansson, M. Krol, A. Lauer, J. Lamarque, X. Liu, V. Montanaro, G. Myhre, J. Penner, G. Pitari, S. Reddy, P. Stier, T. Takemura, and X. Tie, The effect of harmonized emissions on aerosol properties in global models an aerocom experiment, Atmos. Chem. Phys., 7, 4489–4501, 2007.

Tsigaridis, K., Balkansky. Y., Schulz, M., and Benedetti A., 2008: Global error maps of aerosol optical properties: An error propagation analysis, Atmos. Chem. Phys. Discuss., 8, 16027-16059

Toon O.B. and T. P. Ackerman, "Algorithms for the calculation of scattering by stratified spheres," Appl. Opt. 20, 3657-3660 (1981)

Quaas, J., Y. Ming, S. Menon, T. Takemura, M. Wang, J.E. Penner, A. Gettelman, U. Lohmann, N. Bellouin, O. Boucher, A. M. Sayer, G.E. Thomas, A. McComiskey, G. Feingold, C. Hoose, J.E. Kristjánsson, X. Liu, Y. Balkanski, L.J. Donner, P.A. Ginoux, P. Stier, J. Feichter, I. Sednev, S.E. Bauer, D. Koch, R.G. Grainger, A. Kirkevåg, T. Iversen, Ø. Seland, R. Easter, S.J. Ghan, P.J. Rasch, H. Morrison, J.-F. Lamarque, M.J. Iacono, S. Kinne, M. Schulz. Aerosol indirect effects – general circulation model intercomparison and evaluation with satellite data, submitted to ACPD

van der Werf, G. R., Randerson, J. T, Collatz, G. C., and Giglio, L.: Carbon emissions from fires in tropical and subtropical ecosystems, Global Change Biology, 9(4), 547–562, 2003.

Tables

Table 1 Populations, constituents, and possible particle mixing state considerations in the radiation calculations: homogeneously internally mixed (HI), externally mixed (EM), core shell particles (CS).

population description	symbol	constituents	mixing state
sulfate Aitken mode	AKK	SO_4^{-2}, NO_3^-, H_2O	EM/ HI
sulfate accum. mode	ACC	SO_4^{-2}, NO_3^-, H_2O	EM / HI
dust accum. mode (≤%5 inorg.)	DD1	dust, SO_4^{-2}, NO_3^-, H_2O	EM
dust accum. mode (>%5 inorg.)	DS1	dust, SO_4^{-2}, NO_3^-, H_2O	EM / HI
dust coarse mode (≤%5 inorg.)	DD2	dust, SO_4^{-2}, NO_3^-, H_2O	EM
dust coarse mode (>%5 inorg.)	DS2	dust, SO_4^{-2}, NO_3^-, H_2O	EM / HI
sea salt accum. mode	SSA	sea salt, SO_4^{-2}, NO_3^-, H_2O	EM / HI
sea salt coarse mode	SSC	sea salt, SO_4^{-2}, NO_3^-, H_2O	EM / HI
organic carbon (OC)	OCC	OC, SO_4^{-2}, NO_3^-, H_2O	EM / HI
Black carbon (BC) (≤5% inorg.)	BC1	BC, SO_4^{-2}, NO_3^-, H_2O	EM / HI or CS
BC (5–20% inorg.)	BC2	BC, SO_4^{-2}, NO_3^-, H_2O	EM / HI or CS
BC (>20% inorg.)	BC3	BC, SO_4^{-2}, NO_3^-, H_2O	HI or CS
BC – OC	BOC	BC, OC, SO_4^{-2}, NO_3^-, H_2O	HI or CS
BC-sulfate (formed by coagulation)	BCS	BC, SO_4^{-2}, NO_3^-, H_2O	HI or CS
BC-mineral dust	DBC	dust, BC, SO_4^{-2}, NO_3^- , H_2O	HI
mixed	MXX	dust, sea salt, BC, OC, SO_4^{-2}, NO_3, H_2O	HI

Table 2 Emission sizes, geometric mean diameters in [μm], of carbonaceous aerosols.

	OC [OCC] fossil & biofuel	BC [BC1] fossil & biofuel	BC-OC [BOC] biomass burning
S1	0.01	0.01	0.025
S2 (BASE)	0.05	0.05	0.10
S3	0.1	0.1	0.25
S4	0.5	0.5	1

Table 3 Global annual average values for the aerosol direct effect. Aerosol radiative forcing (ARF) at the TOA and at the surface, and surface air temperature.

	ARF_{toa} ACC PD	ARF_{toa} OCC PD	ARF_{toa} BC-SU PD	ARF_{toa} BC-OC PD	ARF_{toa} total PD	IE PD- PI	ARF_{toa} PD - PI	NR PD - PI
BASE	-0.05	-0.22	0.05	0.05	-1.99	-0.45	-0.17	-0.56
R1	-0.05	-0.21	0.05	1.54	-0.51	-0.60	1.01	0.49
R2	-0.05	-0.21	0.05	1.27	-0.78	-0.54	0.81	0.35

Table 4 Statistical analysis between model simulations and EMEP and IMPROVE surface BC concentrations, and AERONET absorption optical thickness and optical thickness. Correlation coefficients, r, and mean values, M, are given. Multi year annual mean data on a monthly basis are used for the EMEP and IMPROVE, 864 and 660 data points, respectively. Year 2000 AERONET data are used as seasonal average resulting in 292 data points. Model data are averaged at station locations.

	EMEP		IMPROVE		AERONET			
	BC mass at surface [$\mu g/m^3$]				AAOT		AOT	
	r	M	r	M	r	M	r	M
Observation		**0.65**		**0.29**		**0.018**		**0.19**
BASE	0.21	0.41	0.53	0.16	0.50	0.014	0.67	0.16
S1	0.18	0.43	0.52	0.17	0.53	0.018	0.63	0.19
S3	0.21	0.38	0.52	0.14	0.55	0.010	0.70	0.14
S4	0.24	0.31	0.45	0.12	0.50	0.008	0.65	0.11
CS	0.20	0.42	0.52	0.16	0.60	0.023	0.66	0.16
CS10	0.18	0.44	0.52	0.16	0.57	0.021	0.65	0.16

Table 5 Global mean budgets of the BASE experiment, for present day conditions (PD), differences between PD and PI, and differences between BASE run and BC reduction experiments under PD conditions. The following variables are listed: Non-biomass burning BC and OC emissions, ($\otimes$ Biomass burning emissions are 3 Tg/a BC and 34.2 Tg/a OC for present-day and 1. T/g BC and 12.7 Tg/a OC for pre-industrial times), CDNC (cm^3), Liquid water path [g/m^2], total cloud cover [%], the indirect effect (IE), aerosol forcing (ARF) at the surface and TOA, and total net radiative change (NR) [W/m^2].

|	BC1 Emission [Tg/a]	OCC Emission [Tg/a]	CDNC [cm^3]	LWP [g/m^2]	Cloud Cover [%]	IE $_{TOA}$ [W/m^2]	ARF $_{surf}$ [W/m^2]	ARF $_{TOA}$ [W/m^2]	NR $_{TOA}$ [W/m^2]
BASE (PD)	4.6	30.9	162	0.702	60.1		-5.11	-1.99	-1.749
			Δ	Δ	Δ	Δ	Δ	Δ	Δ
BASE (PI-PD) $^{\otimes}$	0.4	20.4	41	0.007	0.2	-0.45	-1.39	-0.17	-0.56
BC_50 (PD)	2.3	30.9	4	0.0	-0.05	0.11	0.12	-0.14	-0.03
BCFF (PD)	1.6	30.9	3	-0.001	-0.07	-0.05	0.20	-0.15	-0.19
BCOCBF (PD)	3.0	21.9	-5	-0.003	-0.14	0.20	0.22	-0.07	0.12
BC_diesel(PD)	3.3	30.3	2	0.001	0	-0.05	0.10	-0.05	-0.10

FIGURES
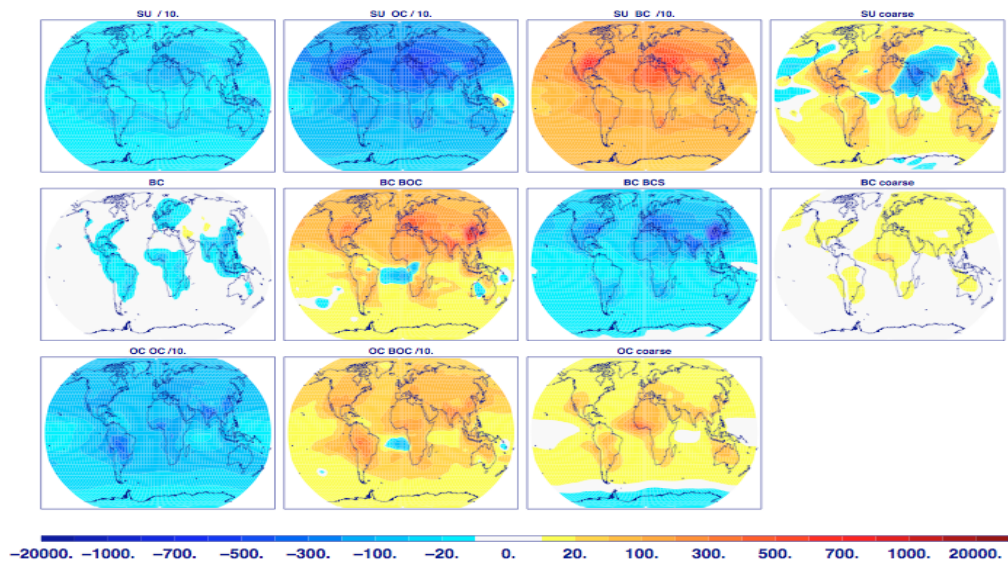
Figure 1. Differences in present day total column aerosol mass concentrations [μg/m2] per mixing state between experiment BA and S1 (S1–BA). The first row shows externally mixed sulfate (population ACC and AKK), sulfate predominantly mixed with OC (OCC, BOC), BC (BC1, BC2, BC3, BCS), and sulfate mixed with coarse aerosols (DS1, DS2, SSC, MXX). Rows two and three show the corresponding changes in mixing state for BC and OC mixtures. Some aerosol concentrations are divided by a factor of ten to match the color bar as indicated in the individual title of the map.

BA – S1
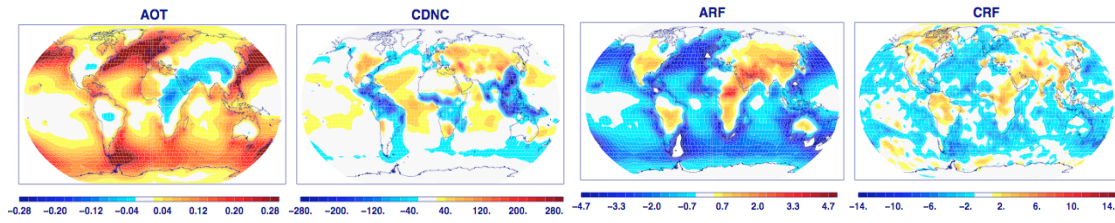
BA – S3
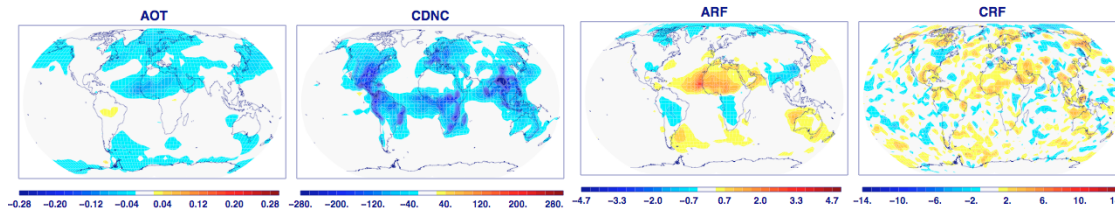
Figure 2 Changes between BA and S1 (S1-Ba) (upper panels) and (BA – S3) (lower panels) for AOT, CDNC [column mean #/cm^3], ARF [W/m^2] and CRF [W/m^2]. All maps are showing differences between the experiments for present day conditions.
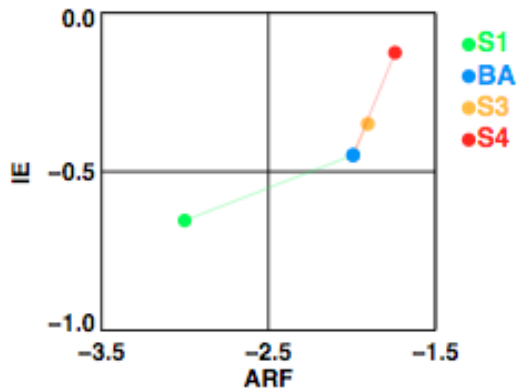
Figure 3 Global mean IE and ARF [W/m^2] values for all size experiments, (S1 – 4) and the base experiment, BA, for present day conditions.
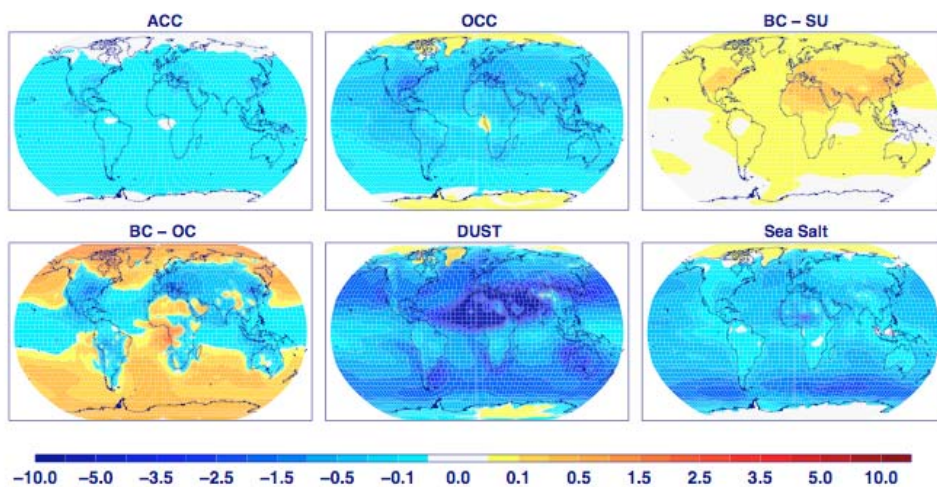
Figure 4 Present day radiative forcing at the top of the atmosphere by species for the BA experiment. Externally mixed sulfates and nitrates (ACC), organics (OCC), black carbon/ sulfate/nitrate mixture (BC – SU), black carbon/organic carbon mixture (BC – OC), dust and sea salt. Units are [W/m^2].
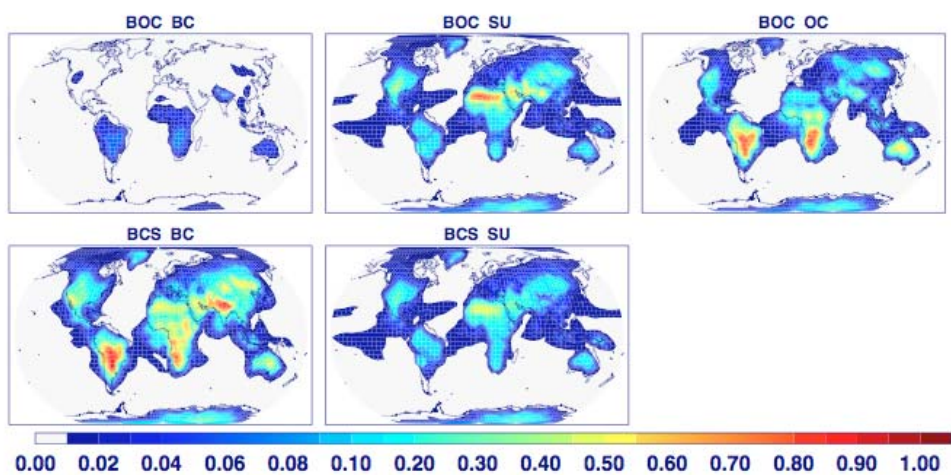
Figure 5 Fractional contributions of BC, sulfate and OC, in population BOC (upper row), and BCS (lower row). Aerosol water is not displayed.
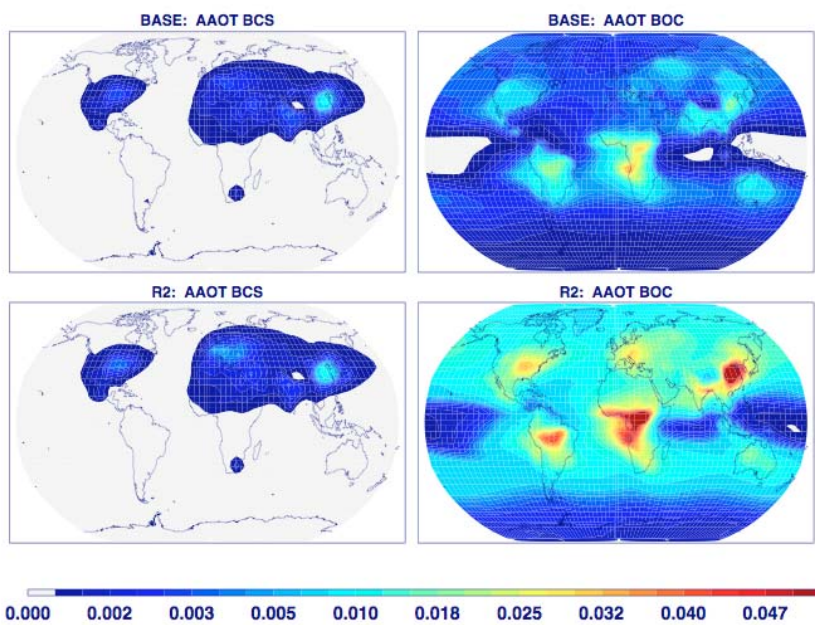
Figure 6 Absorption optical thickness of BC – sulfate mixtures (left column), and BOC (right column), for experiments BASE and R2.
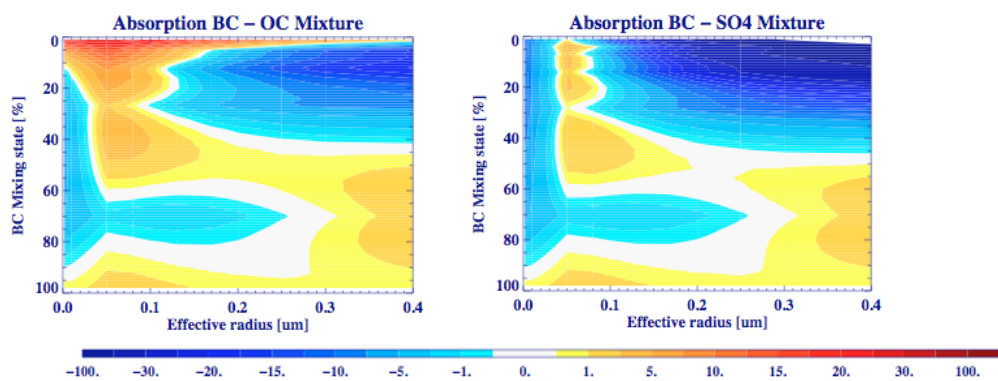
Figure 7 Percentage difference in absorption between a homogeneous mixing calculation and a core-shell Mie calculations, for BC cores with OC coating (left) and sulfate coating (right).
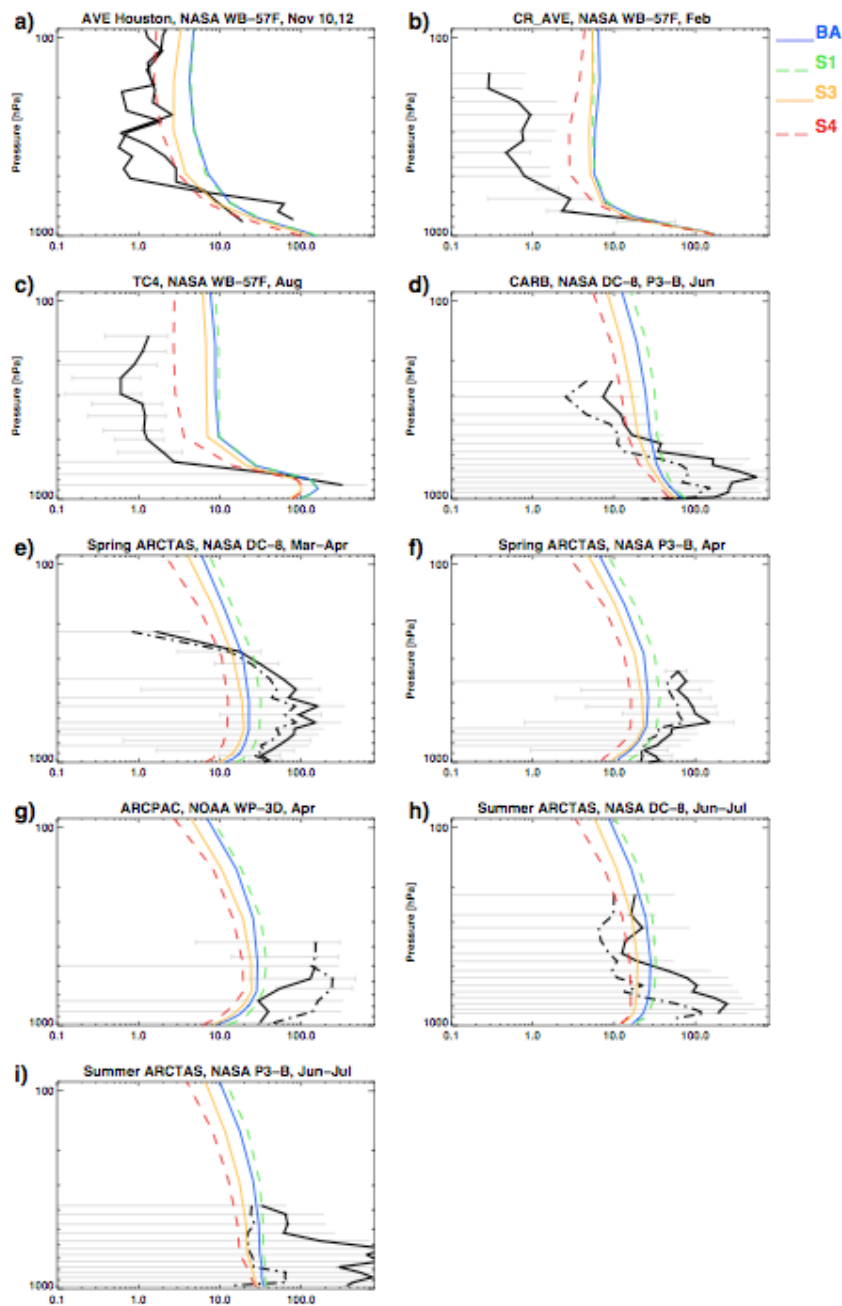
Figure 8 Modeled (colored) and observed (black lines) BC mass profiles in [ng/kg] in the tropics and mid-latitudes (a–d) and ARCPAC and ARCTAS campaign (e–i). Observations are averaged for the respective campaigns, with standard deviations where available. The two black lines in Fig a) show measurements on two different days. All other profiles give multiple day averages. Mean (solid) and median (dashed) observed profiles are provided except for (g) the ARCPAC campaign has distinct profiles for the mean of the 4 flights that probed long-range biomass burning plumes (dashed) and mean for the1flight that sampled aged Arctic air (solid).

34
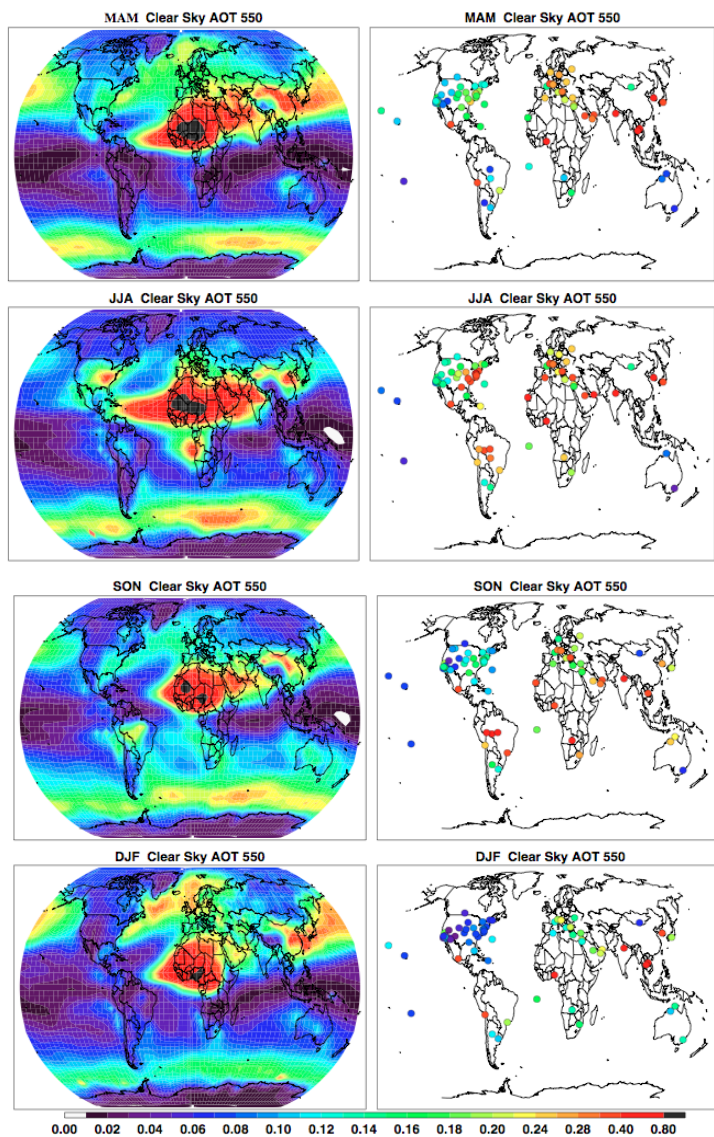
Figure 9 Aerosol optical thickness at 550 nm for clear sky conditions shown for the four seasons. Left column shows model data and in te right column, filled circles give AERONET data.
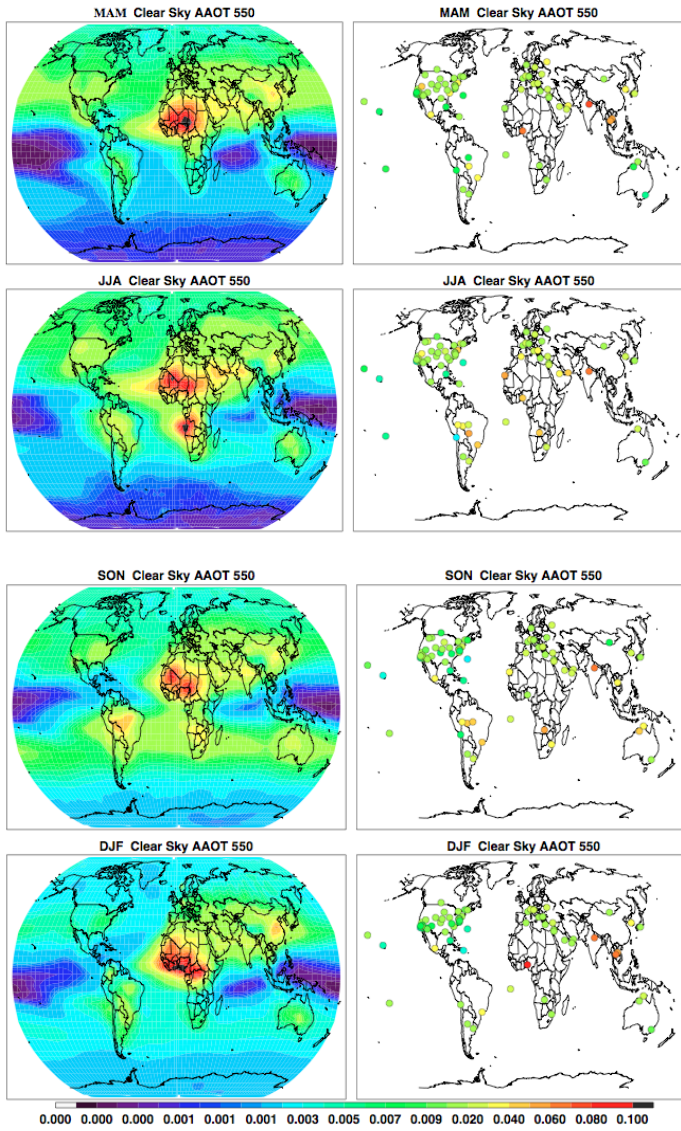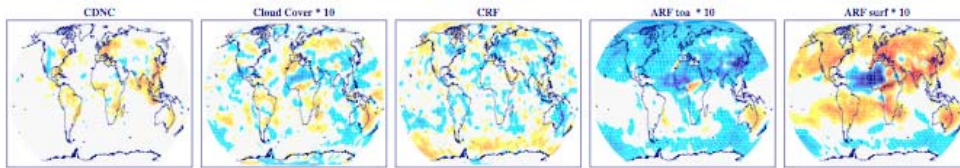
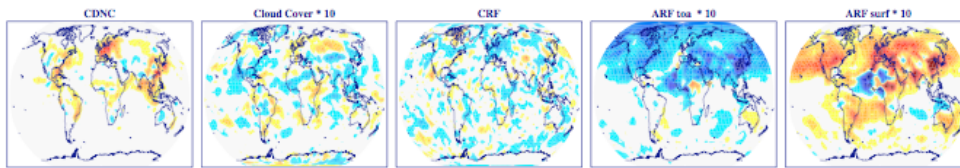**Figure 10** Absorption optical thickness at 550 nm. Filled circles give AERONET data.

BASE PI - PD
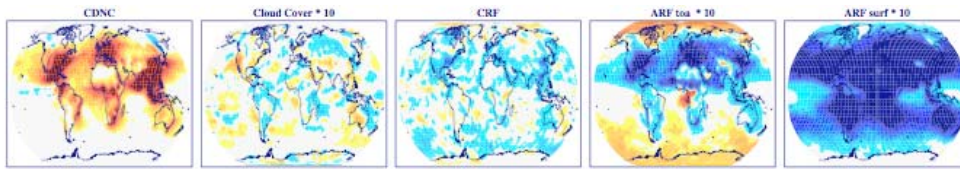
BC_50

BCFF

BCOCBF

BC_diesel

−140. −100. −60. −20. 20. 60. 100. 140.   −14. −12. −10. −8. −6. −4. −2. 0. 2. 4. 6. 8. 10. 12. 14.
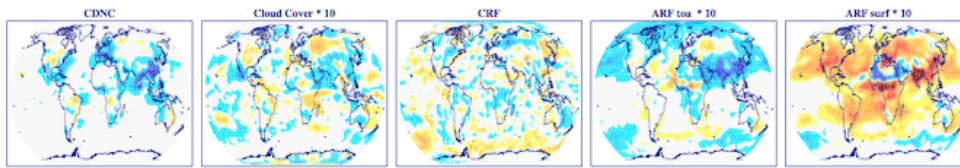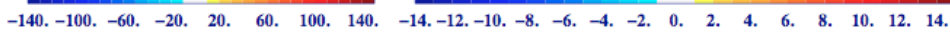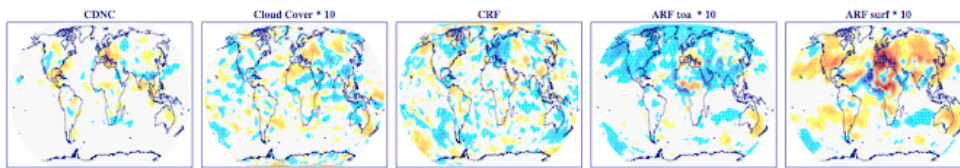
Figure 11 Differences in CDNC [cm^3], total cloud cover [%], top of the atmosphere cloud (CRF), aerosol (ARF) and surface aerosol forcing [W/m^2], between the PD and PI in the BASE case (first panel) and the difference between BASE and the four BC reduction cases.